

# Enhanced thermal conductivity of ethylene glycol with single-walled carbon nanotube inclusions

S.Harish<sup>1</sup>, Kei Ishikawa<sup>1</sup>, Erik Einarsson<sup>1,2</sup>, Shinya Aikawa<sup>1,3</sup>, Shohei Chiashi<sup>1</sup>,  
Junichiro Shiomi<sup>1</sup>, Shigeo Maruyama<sup>1\*</sup>

<sup>1</sup>Department of Mechanical Engineering, The University of Tokyo, 7-3-1 Hongo, Bunkyo-ku,  
Tokyo 113-8656, Japan

<sup>2</sup>Global Center of Excellence for Mechanical Systems Innovation, The University of Tokyo,  
7-3-1 Hongo, Bunkyo-ku, Tokyo 113-8656, Japan

<sup>3</sup>Department of Electrical Engineering, Tokyo University of Science, 1-3 Kagurazaka, Shinjuku-ku,  
Tokyo 162-8601, Japan

# Enhanced thermal conductivity of ethylene glycol with single-walled carbon nanotube inclusions

## Abstract

In the present work, we report measurements of the effective thermal conductivity of dispersions of single-walled carbon nanotube (SWNT) suspensions in ethylene glycol. The SWNTs were synthesized using the alcohol catalytic chemical vapour deposition method. Resonant Raman spectroscopy was employed to estimate the diameter distribution of the SWNTs based on the frequencies of the radial breathing mode peaks. The nanofluid was prepared by dispersing the nanotubes using a bile salt as the surfactant. Nanotube loading of up to 0.3 wt% was used. Thermal conductivity measurements were performed by the transient hot-wire technique. Good agreement, within an uncertainty of 2%, was found for published thermal conductivities of the pure fluids. The enhancement of thermal conductivity was found to increase with respect to nanotube loading. The maximum enhancement in thermal conductivity was found to be 14.8% at 0.3 wt% loading. The experimental results were compared with literature results in similar dispersion medium. Experimental results were compared with the Hamilton-Crosser model, the Lu-Lin model, Nan's effective medium theory and the Hashin-Strikman model. Effective medium theory seems to predict the thermal conductivity enhancement reasonably well compared to rest of the models. Networking of nanotubes to form a tri-dimensional structure was considered to be the reason for the thermal conductivity enhancement.

**Keywords:** Nanofluids, Single-walled carbon nanotube, Thermal conductivity.

## 1. INTRODUCTION

Conventional heat transfer fluids exhibit poor heat transfer performance due to their low thermal conductivities. Many research activities have been carried out in the past to improve the thermal properties of these fluids by seeding a small quantity of highly thermally conductive solid in it [1]. However, this has not been very successful because of settling of the solid particles due to their large size [1]. Recent developments in the field of nanoscience have led to the development of a new class of fluids termed “nanofluids” [2]. Over the past decade, nanofluids—colloidal dispersions prepared by uniformly dispersing nanostructures such as nanoparticles, nanotubes and nanofibers in conventional heat transfer fluids—have gained attraction worldwide because of their superior thermal performance [2-5]. Many research groups experimentally reported a substantial increase in the thermal conductivity [3] and the convective heat transfer coefficient [4] of such fluids.

Nanoparticles of various metals and metal oxides have been used for nanofluid production. These predominantly include copper, copper oxide, aluminum, aluminum oxide, Zinc oxide, titanium dioxide, etc. [3,5] More recently, a significant number of studies have made use of carbon-based nanostructures, namely graphite [6], fullerene [7], single-walled carbon nanotubes (SWNTs) [8], multi-walled carbon nanotubes (MWNTs) [9-20], nano diamond [21] and graphene [22, 23] to prepare nanofluids. Recent studies reveal that carbon nanotubes have very high thermal conductivity [24-28], hence it is obvious to expect that the suspensions consisting of nanotubes/grapheme sheets would show higher thermal conductivity enhancement compared to other nanoparticles.

The first experimental observation of thermal conductivity enhancement was reported by Choi and co-workers for the case of MWNTs dispersed in poly-( $\alpha$  olefin) oil [9]. They reported an enhancement of 160% at a nanotube loading of 1 vol%. This huge enhancement, however, could not be reproduced by subsequent studies [10-19]. Despite such a large discrepancy in the experimental results, all the results were found to be significantly higher than those predicted by analytical

models. Therefore, more studies need to be performed to measure the effective thermal conductivity of nanotube suspensions in different base fluids.

In the present work, we report the effective thermal conductivity of SWNT suspensions in ethylene glycol (EG). We also compare the measured effective thermal conductivity with existing analytical models to determine which model is in best agreement with the experimental observations.

## **2. MATERIALS AND METHODS**

### ***2.1 Material synthesis***

SWNTs were synthesized by the catalytic chemical vapour deposition (CVD) technique using ethyl alcohol as the carbon source as described by Maruyama et al. [29] Cobalt and iron catalysts supported with zeolite were employed. Amorphous carbon impurities and metal particle impurities were dramatically suppressed at the reaction temperature of 800°C. The etching effect caused by the decomposed hydroxyl (-OH) radical, which removes carbon atoms with dangling bonds during the CVD process was reported as the reason for the high purity of the SWNTs [29]. A transmission electron microscopy (TEM) image of the ‘as grown’ SWNTs from ethanol feedstock is shown in Figure 1.

### ***2.2 Characterization by Resonant Raman Spectroscopy***

Resonant Raman spectra (RRS) of the ‘as grown’ SWNT sample were acquired using a macro-Raman apparatus with a 50 cm single monochromator and a CCD detector. The excitation wavelength used was 488 nm with an Argon ion laser.

A typical RRS obtained from the SWNT sample is shown in Figure 2. The low frequency features (100-400  $\text{cm}^{-1}$ ) show the Radial Breathing Mode (RBM) peaks, the frequencies of which are dependent on the SWNT diameter. The G-band observed around 1592  $\text{cm}^{-1}$  is the characteristic

feature of the graphitic layers, and corresponds to in-plane vibrations of the carbon atoms. In addition to the G-band and RBM, the D-band observed near  $1350\text{ cm}^{-1}$  arises from defects in the graphitic structure. A high ratio of the intensities of the G band and D-band ( $I_G/I_D$ ) reveal that the purity of the bulk sample is very high [30].

The expanded RBM signal along with the diameter distribution is shown in the inset of Figure 2. The RBM frequency ( $\omega_{\text{RBM}}$ ) is proportional to the inverse of the nanotube diameter, following the equation  $\omega_{\text{RBM}} = A/d + B$ , where  $d$  is the diameter of the nanotube, and  $A$  ( $\text{cm}^{-1}\text{ nm}$ ) and  $B$  ( $\text{cm}^{-1}$ ) are constants [30]. The parameters  $A$  and  $B$  are typically determined experimentally, and for the present case the commonly used values of 248 and 0 were used for  $A$  and  $B$  respectively [29-31]. From the expanded RBM signal shown in figure 2, the typical diameter distribution of the SWNT samples synthesized using ethanol feedstock was estimated to be 0.8-1.4 nm.

### ***2.3 Nanofluid preparation***

The highly hydrophobic nature of SWNTs makes it very difficult to disperse them in a liquid medium. An important prerequisite for the nanofluid is the preparation of a stable and homogenous suspension. Two popular techniques prevail in the open literature for creating stable dispersions. The first technique is to attach a hydrophilic functional group onto the nanotube sidewalls by strong acid treatment [10]. The other method is to encapsulate the SWNTs using polar surfactants. Though acid treatment is frequently used to disentangle MWNTs, it may not be very suitable for SWNTs as it will heavily damage the sidewalls [32]. In our present work, we made use of a surfactant to prepare the nanofluid dispersion.

The commonly used surfactant in the nanofluid preparation are sodium dodecylbenzene sulphonate (SDBS) [14], Sodium dodecyl sulfate (SDS) [11], Gum Arabic [12], hexadecyltrimethylammonium bromide (CTAB) [33], and Octyl phenol ethoxylate (Triton-X100) [34]. Wenseleers et al. reported the potential of using sodium deoxycholate (SDC), a bile salt, as a dispersion agent for SWNTs

[35]. For the present experiments, SDC was chosen as the surfactant to make SWNT/EG dispersions.

The structure of SDC is shown in Figure 3. SDC possess a rigid structure consisting of a cholesterol group with dissimilar sides [36]. It consists of a steroid skeleton with a carboxylic acid side chain at one end and two hydroxyl groups on its steroid backbone. The two polar hydroxyl groups on the  $\alpha$ -face and methyl group on the other side facilitate strong adsorption of the SDC onto the surface of SWNTs [36, 37].

The stable dispersions were prepared by adding the necessary loading of SWNTs in ethylene glycol and then 0.5 w/v % of the surfactant. The density of the SWNTs used for calculation purpose was  $1.6 \text{ g/cm}^3$  [38]. The dispersions were subjected to bath sonication for 90 minutes followed by tip sonication using an ultrasonic processor (Hielscher GmbH, UP-400S with H3/Micro Tip 3) for 120 minutes at a power flux level of  $368 \text{ W/cm}^2$  (80% amplification). The pH of the dispersion was 7. The length of the nanotubes after sonication from our Atomic Force Microscopy (AFM) measurements was found to be between 150 nm – 500 nm.

#### ***2.4 Thermal conductivity measurement setup***

In the present study we make use of the transient hot wire (THW) technique to measure the thermal conductivity of the nanofluids. A platinum (Pt) hot wire of 10  $\mu\text{m}$  diameter and 20 mm length is placed inside the test cell. The Pt wire acts as both the heater and an electrical resistance thermometer. This technique is based on the measurement of temperature and temporal response of the hot wire when it is subjected to an electrical pulse.

The relation between thermal conductivity  $k$  and measured temperature  $T$  can be summarized as follows [39]. Assuming a thin, infinite line heat source with constant heat output in an infinite medium, the energy equation can be written as

$$\frac{1}{\alpha} \frac{\partial T}{\partial t} = \frac{1}{r} \frac{\partial}{\partial r} \left( r \frac{\partial T}{\partial r} \right) \quad (1)$$

With initial condition and boundary conditions

$$T(t = 0) = T_0 \quad (2)$$

and

$$lt \left( r \frac{\partial T}{\partial r} \right) = \frac{q}{2\pi k} \text{ and } \frac{\partial T}{\partial r} = 0 \quad (3)$$

the analytical solution is of the form

$$T(r, t) = T_0 + \frac{q}{4\pi k} \left\{ -\gamma + \ln\left(\frac{4\alpha t}{r^2}\right) + \dots \right\} \quad (4)$$

Here,  $\alpha$  is the thermal diffusivity and  $\gamma=0.5772$  is Euler's constant. If the temperature of the hot wire at times  $t_1$  and  $t_2$  were  $T_1$  and  $T_2$  respectively, then by eliminating the higher order terms in Eq. (4), the thermal conductivity of the fluids can be approximated in the following form:

$$k = \frac{q}{4\pi} \frac{\ln(t_1/t_2)}{T_1 - T_2} \quad (5)$$

During the experiments, the Pt wire is heated with the aid of a constant DC power supply. The temperature rise of the hot wire is determined from the change in resistance of the hot wire, which can be measured in time using a Wheatstone-bridge circuit. With known electric power supply and slope of the curve  $\ln(t)$  versus  $T$ , the thermal conductivity  $k$  is calculated using equation (5).

### ***2.5 Calibration of the THW setup and uncertainty analysis***

To validate the THW setup, the thermal conductivity of pure deionized water and ethylene glycol were measured at different temperatures. A comparison of the measured and reference thermal conductivity data is shown in Figure 4. The upper line corresponds to the thermal conductivity of water according to the ASTM-D2717 standard [40]. The lower line corresponds to the thermal conductivity of EG reported by Di Giulio & Teja [41].

The measured results were in good agreement with the reference data reported in the literature. A detailed uncertainty analysis of the THW setup based on the method prescribed by [42, 43] was carried out, and the experimental uncertainty was found to be  $\pm 2\%$ .

### **3. RESULTS AND DISCUSSION**

#### ***3.1 Experiments***

Thermal conductivities of the SWNT-dispersed EG samples were measured for different SWNT loadings ranging from 0.1 to 0.3 wt% using the THW setup. Figure 5 shows the thermal conductivities versus different SWNT loadings measured at room temperature. The thermal conductivity increased with increasing SWNT loading in a linear fashion. At a loading of 0.1 wt% no significant improvement in effective conductivity was obtained (only 2.7%). This minor increase lies very well within the experimental uncertainty limits and cannot be considered as conductivity enhancement. However, on further increasing the nanotube loading, a significant improvement in the effective conductivity was measured. A maximum enhancement of 14.8% at a loading of 0.3 wt% was found in this study.

The results of this study show thermal conductivity enhancements are less than those reported by Choi et al [9] for poly-( $\alpha$  olefin) oil. Xie et al. [10], Liu et al. [13] and Lamas et al. [18] reported enhancements of 12.7%, 12.4% and 11.5% respectively at 1 vol% loading. Ruan and Jacobi recently reported an enhancement of 9.3% at a volume fraction of 0.24% for EG/MWNT nanofluids [20]. Yu et al. reported an enhancement of 18% for nano-diamond-based nanofluids at 1 vol% [16]. Nanda et al. reported an enhancement of 36% at for SWNT/EG nanofluids at 1 vol% [21]. Baby and Ramaprabhu [23] developed graphene-based nanofluids and reported an enhancement of up to 7% at a very low loading of 0.05 vol%. Eastman et al. [44] reported an enhancement of 40% at 0.3 vol% for Copper/EG based nanofluids. In this work, such a high enhancement was not observed. The magnitude of effective thermal conductivity enhancement for EG-based nanofluids reported in



this work is in consistent with the existing literature data, however at different nanotube concentrations. This difference could be attributed to the aspect ratio of the material used, purity level, and treatment method adopted to prepare the nanofluid dispersion.

### ***3.2 Comparison with theoretical models***

The experimental results are compared with the Hamilton-Crosser model (H-C) [45], the Lu-Lin model [46], Nan's effective medium theory [47-48] and the Hashin-Strikman model (H-S) [49]. For the present theoretical calculations, fluid thermal conductivity of  $0.252 \text{ Wm}^{-1}\text{K}^{-1}$ , SWNT thermal conductivity of  $1750 \text{ Wm}^{-1}\text{K}^{-1}$  [24], an aspect ratio (length to diameter ratio) of 300, and interfacial resistance of  $10^{-8} \text{ m}^2\text{K/W}$  [50] were taken for calculations.

Figures 6 and 7 show the comparison of the above models with the present experimental results. The horizontal axes have been converted to volume concentration instead of weight concentration for comparison with other reports. It can be seen from Figure 6 that the Hamilton-Crosser model and Lu-Lin model completely underestimate the effective conductivity at all concentrations. Nan's effective medium theory completely overestimates the effective conductivity when the interfacial thermal resistance is not taken into account. However, when the influence of interfacial thermal resistance is taken into account, Nan's model underestimates the effective conductivity but still performs much better than the H-C and Lu-Lin models. Hence, it can be said that the large thermal resistance across the interface plays a significant role in reducing the effective conductivity of the nanofluid. For the present experiments, interfacial thermal resistance was found to be  $2.4 * 10^{-9}$  by fitting the experimental data which is one order of magnitude higher than the one reported by Huxtable et al. [50]. It may be possible that the interface resistance varies depending on the surfactant used and the dispersion medium. Lack of clear knowledge about the interfacial thermal resistance remains a hindrance to completely rely on this model. However, it helps to understand

the critical role of interfacial thermal resistance in the degradation of thermal conductivity enhancement.

Figure 7 shows the theoretical bounds of the H-S model along with the present experimental and literature results. In two recent studies, Fan and Wang [51, 52] argued that when the ratio of the thermal conductivity of the nanomaterial to the base fluid conductivity is greater than unity, the separation between upper and lower limits of this model becomes more pronounced. They also found that particles with higher conductivities tend to interconnect and disperse in the base fluid. As a result, the energy transport across the interface is greatly enhanced, making it possible for the nanofluids to achieve remarkable enhancements as predicted by the upper bound of the H-S model by simply tuning the morphology of the nanomaterial [51, 52].

The majority of the experimental data in the prevailing literature fit very well within the upper and lower limits set by the present model [52]. However, for the case of carbon nanotubes, the upper bound set by this model is exceptionally high. This model has a major drawback that it fails to take interfacial thermal resistance into account. Further work need to be carried out in the future to improve this model or to develop a new model to accurately estimate the thermal conductivity of carbon nanotube-based nanofluids.

The mechanism behind the thermal conductivity enhancement also remains unclear. Many mechanisms, such as Brownian motion, micro convection, formation of ordered liquid layer, ballistic motion and particle clustering have been proposed to explain the conductivity enhancement [3, 5]. Tsai et al. [53] reported that in high viscous fluids Brownian motion is greatly inhibited. Hence, it is unlikely that Brownian motion and Brownian motion assisted micro convection are responsible for the conduction enhancement noticed in this work. In the presence of surfactant-encapsulated nanotubes, the formation of an ordered liquid layer is difficult [14]. The enhancement observed in the present work can be attributed to the percolation of the CNTs to form a network [14, 54]. However, experimental evidence for this mechanism is still lacking. Further

experiments also need to be carried out to determine the underlying mechanism behind the thermal conductivity enhancement noticed in nanofluids.

#### **4. CONCLUSIONS**

Single walled carbon nanotubes were synthesized the by alcohol catalytic chemical vapour deposition method, and nanofluid dispersions were created using a bile salt as the surfactant. The effective thermal conductivity of the nanofluids was measured using the transient hot wire technique. The effective thermal conductivity increased in linear fashion with respect to the nanotube loading. Classical models failed to predict the experimental results. Hashin-Strikman model sets very unrealistic upper bound for the thermal conductivity enhancement. Effective medium theory seems to perform better than rest of the models. Formation of networking structure was considered to be the potential reason behind the conductivity enhancement observed. However, further work need to be carried out to provide experimental evidence to explain the mechanism behind the heat conduction in nanofluids.

#### **Acknowledgments**

Part of this work was financially supported by Grant-in-Aid for Scientific Research (22226006, 22246023 and 19054003). Part of this work was supported financially by the Japanese Government Monbukagakusho (MEXT) Scholarship and the “Global Center of Excellence for Mechanical Systems Innovation” (GMSI). The authors acknowledge the help of C. Kramberger at the University of Tokyo for helpful discussions about Raman characterization.

#### **References**

- [1] A.S. Ahuja, Augmentation of heat transfer in laminar flow of polystyrene suspensions, *Journal of Applied Physics* 46 (8) (1975) 3408-3416.

- [2] S.U.S. Choi, Enhancing thermal conductivity of fluids with nanoparticles, in: D.A. Siginer, H.P. Wang, (Eds.), *Developments and Applications of Non-Newtonian Flows*, ASME, New York, FED-Vol. 231/MD-Vol. 66, 1995, pp. 99–105.
- [3] J. Fan, L. Wang, Review of heat conduction in nanofluids, *Journal of Heat Transfer* 133 (4) (2011) 040801-1-14.
- [4] W. Daungthongsuk, S. Wongwises, A critical review of convective heat transfer of nanofluids, *Renewable and Sustainable Energy Reviews* 11 (3) (2007) 797-817.
- [5] C. Kleinstreuer, Y. Feng, Experimental and theoretical studies of nanofluid thermal conductivity enhancement: a review, *Nanoscale Research Letters* 6 (2011) 229-241.
- [6] Y. Yang, Z.G. Zhang, E.A. Grulke, W.B. Anderson, G. Wu, Heat transfer properties of nanoparticles-in fluid dispersions (nanofluids) in laminar flow, *International Journal of Heat and Mass Transfer* 48 (6) (2005) 1107-1116.
- [7] Y. Hwang, J.K. Lee, C.H. Lee, Y.M. Jung, S.I. Cheong, C.G. Lee, B.C. Ku, S.P. Jang, Stability and thermal conductivity characteristics of nanofluids, *Thermochimica Acta* 455 (1-2) (2007) 70-74.
- [8] J. Nanda, C. Maranville, S.C. Bollin, D. Sawall, H. Otani, J.T. Remillard, J.M. Ginder, Thermal conductivity of single-wall carbon nanotube dispersions: role of interfacial effects, *Journal of Physical Chemistry C* 112 (3) (2008), 654-658.
- [9] S.U.S. Choi, Z.G. Zhang, W. Yu, F.E. Lockwood, E.A. Grulke, Anomalous thermal conductivity enhancement in nanotube suspensions, *Applied Physics Letters* 79 (14) (2001) 2252-2254.
- [10] H. Xie, H. Lee, W. Youn, M. Choi, Nanofluids containing multi-walled carbon nanotubes and their enhanced thermal conductivities, *Journal of Applied Physics* 94 (8) (2003) 4967-4971.
- [11] M.J. Assael, C.F. Chen, I. Metaxa, W.A. Wakeham, Thermal conductivity of suspensions of carbon nanotubes in water, *International Journal of Thermophysics* 25 (4) (2004) 971-985.

- [12] Y. Ding, H. Alias, D. Wen, R.A. Williams, Heat transfer of aqueous suspensions of carbon nanotubes (CNT nanofluids), *International Journal of Heat and Mass Transfer* 49 (1-2) (2006) 240-250.
- [13] M.S. Liu, M.C.C. Lin, I.T. Huang, C.C. Wang, Enhancement of thermal conductivity with carbon nanotube for nanofluids, *International communications in Heat and Mass Transfer* 32 (9) (2005) 1202-1210.
- [14] D. Wen, Y. Ding, Effective thermal conductivity of aqueous suspensions of carbon nanotubes, *Journal of Thermophysics and Heat Transfer* 18 (4) (2004) 481-485.
- [15] P. Garg, J.L. Alvarado, C. Marsh, T.A. Carlson, D.A. Kessler, K. Annamalai, An experimental study on the effect of ultrasonication on viscosity and heat transfer performance of multi-wall carbon nanotube based aqueous nanofluids, *International Journal of Heat and Mass Transfer* 52 (21-22) (2009) 5090-5101.
- [16] L. Chen, H. Xie, Y. Li, W. Yu, Nanofluids containing carbon nanotubes treated by mechanochemical reaction, *Thermochimica Acta* 477 (1-2) (2008) 21-24.
- [17] H. Xie, L. Chen, Review on the preparation and thermal performances of carbon nanotube contained nanofluids, *Journal of Chemical and Engineering Data* 56 (4) (2011) 1030-1041.
- [18] B.C. Lamas, M.A.L. Fonseca, F.A.M.M. Gonclaves, A.G.M. Ferreira, I.M.A Fonseca, S. Kanagaraj, N. Martins, M.S.A. Oliveira, EG/CNTs nanofluids engineering and thermo-rheological characterization, *Journal of Nano Research* 13 (2011) 69-74.
- [19] T. Phuoc, M. Massoudi, R.H. Chen, Viscosity and thermal conductivity of nanofluids containing multi-wall carbon nanotubes stabilized by chitosan, *International Journal of Thermal Sciences* 50 (1) (2011) 12-18.
- [20] B. Ruan, A.M. Jacobi, Intertube falling-film heat transfer behaviour of multi-wall carbon nanotube suspensions (MWNT nanofluids), *Proceedings of ASME/JSME 8<sup>th</sup> Thermal Engineering Joint Conference*, 13-17 March 2011, Honolulu, Hawaii, USA.

- [21] W. Yu, H. Xie, Y. Li, L. Chen, Q. Wang, Experimental investigation on the thermal transport properties of ethylene glycol based nanofluids containing low volume concentration diamond nanoparticles, *Colloids and Surfaces A: Physicochemical and Engineering aspects* 380 (1-3) (2011) 1-5.
- [22] W. Yu, H. Xie, X. Wang, X. Wang, Significant thermal conductivity enhancement for nanofluids containing graphene nanosheets, *Physics Letters A* 375 (10) (2011) 1323-1328.
- [23] T.T. Baby, S. Ramaprabhu, Investigation of thermal and electrical conductivity of graphene based nanofluids, *Journal of Applied Physics* 108 (12) (2010) 124308-1-6.
- [24] J. Hone, M. Whitney, C. Piskoti, A. Zettl, Thermal conductivity of single walled carbon nanotubes, *Physical Review B* 59 (4) (1999) R2514-R2516.
- [25] M. Fuji, X. Zhang, H. Xie, H. Ago, K. Takahasi, T. Ikuta, H. Abe, T. Shimizu, Measuring the thermal conductivity of single carbon nanotube, *Physical Review Letters* 95 (6) (2005) 065502-1-4.
- [26] C. Yu, L. Shi, Z. Yao, D. Li, A. Majumdar, Thermal conductance and thermo power of an individual single wall carbon nanotube, *Nano Letters* 5 (9) (2005) 1842-1846.
- [27] E. Pop, D. Mann, Q. Wang, K. Goodson, H. Dai, Thermal conductance of an individual single wall carbon nanotube above room temperature, *Nano Letters* 6 (1) (2006) 96-100.
- [28] T. Choi, D. Poulikakos, J. Tharian, U. Sennhauser, Measurement of the thermal conductivity of individual carbon nanotubes by the four-point three- $\omega$  method, *Nano Letters* 6 (8) (2006) 1589-1593.
- [29] S. Maruyama, R. Kojima, Y. Miyauchi, S. Chiashi, M. Kohno, Low temperature synthesis of high purity single walled carbon nanotubes from alcohol, *Chemical Physics Letters* 360 (3-4) (2002) 229-234.
- [30] R. Saito, G. Dresselhaus, M.S. Dresselhaus, Trigonal warping effect of carbon nanotubes, *Physical Review B* 61 (4) (2000) 2981-2990.

- [31] A. Jorio, R. Saito, J.H. Hafner, C.M. Lieber, M. Hunter, T. McClure, G. Dresselhaus, M.S. Dresselhaus, Structural (n,m) determination of isolated single wall carbon nanotubes by resonant Raman scattering, *Physical Review Letters* 86 (6) (2001) 1118-1121.
- [32] H. Hong, J. Wensel, Heat transfer nanofluids based on carbon nanotubes, *Journal of Thermophysics and Heat Transfer* 21 (1) (2007) 234-236.
- [33] M.J. Assael, I.N. Metaxa, J. Aravinitidis, D. Christofilos, C. Lioutas, Thermal conductivity enhancement in aqueous suspensions of carbon multi walled and double walled nanotubes in the presence of two different dispersions, *International Journal of Thermophysics* 26 (3) (2005) 647-664.
- [34] H. Wang, W. Zhou, D.L. Ho, K.I. Winey, J.E. Fischer, C.J. Glinka, E.K. Hobbie, Dispersing single-walled carbon nanotubes with surfactants: a small angle neutron scattering study, *Nano Letters* 4 (9) (2004) 1789 – 1793.
- [35] W. Wensleers, I.I. Vlasov, E. Goovaerts, E.D. Obraztsova, A.S. Lobach, A. Bouwen, Efficient isolation and solubilization of pristine single-walled nanotubes in bile salt micelles, *Advanced Functional Materials* 14 (11) (2004) 1105-1112.
- [36] N.A. Mazer, M.C. Carey, R.F. Kwanick, G.B. Benedeck, Quasielastic light scattering studies of aqueous biliary lipid systems. Size, shape and thermodynamics of bile salt micelles, *Biochemistry* 18 (14) (1979) 3064-3075.
- [37] F. Bonaccorso, T. Hasan, P.H. Tan, C. Sciascia, G. Privitera, G. Di Marco, P.G. Gucciardi, A.C. Ferrari, Density gradient ultra-centrifugation of nanotubes: Interplay of bundling and surfactants encapsulation, *Journal of Physical Chemistry C* 114 (41) (2010) 17267-17285.
- [38] HiPco technical data sheet, [www.nanointegris.com/en/downloads](http://www.nanointegris.com/en/downloads) 2011.
- [39] H.S. Carsla, J.C. Jaeger, *Conduction of heat in solids*, Oxford University Press, USA, 2<sup>nd</sup> edition, 1986.
- [40] American Society of Testing and Materials, *Standard test method for thermal conductivity of*

liquids, ASTM D-2717 (2009) 95-98.

- [41] R. Di Giulio, A.S. Teja, Thermal conductivity of poly (ethylene glycols) and their binary mixtures, *Journal of Chemical Engineering Data* 35 (2) (1990) 117-121.
- [42] H.W. Coleman, W.G. Steele, *Experimentation and uncertainty analysis for engineers*, Wiley-Interscience, USA, 2<sup>nd</sup> edition, 1999.
- [43] M. Kostic, K.C. Simham, Computerized transient hot wire thermal conductivity apparatus for nanofluids, *Proceedings of the 6<sup>th</sup> WSEAS International Conference on Heat and Mass Transfer*, 10-12 January 2009, Ningbo, China.
- [44] J.A. Eastman, S.U.S. Choi, S. Li, W. Yu, L.J. Thompson, Anomalously increased effective thermal conductivities of ethylene glycol-based nanofluids containing copper nanoparticles, *Applied Physics Letters* 78 (6) (2001) 1341218-1-3.
- [45] R.L. Hamilton, O.K. Crosser, Thermal conductivity of heterogeneous two component systems, *Industrial Engineering and Chemistry Fundamentals* 1 (3) (1962) 187-191.
- [46] S. Lu, H. Lin, Effective conductivity of composites containing aligned spheroidal inclusions of finite conductivity, *Journal of Applied Physics* 79 (9) (1996) 6761-6769.
- [47] C.W. Nan, R. Birringer, D.R. Clarke, H. Gleitzer, Effective thermal conductivity of particulate composites with interfacial thermal resistance, *Journal of Applied Physics* 81 (10) (1997) 6692-6699.
- [48] C.W. Nan, G. Liu, Y. Lin, M. Li, Interface effect on thermal conductivity of carbon nanotube composites, *Applied Physics Letters* 85 (16) (2004) 3549-3551.
- [49] Z. Hashin, S. Shtrikman, Conductivity of polycrystals, *Physical Review* 130 (1) (1963) 129-133.
- [50] S.T. Huxtable, D.G. Cahill, S. Shenogin, L. Xue, R. Ozisik, P. Barone, M. Usrey, M.S. Strano, G. Siddons, M. Shim, P. Keblinski, Interfacial heat flow in carbon nanotube suspensions, *Nature Materials* 2 (2003) 731-734.



- [51] J. Fan, L. Wang, Heat conduction in nanofluids: Structure property correlation, *International Journal of Heat and Mass Transfer* 54 (19-20) (2011) 4349-4359.
- [52] L. Wang, J. Fan, Toward nanofluid of ultra-high thermal conductivity, *Nanoscale Research Letters* 6 (2011) 153-161.
- [53] T.H. Tsai, L.S. Kuo, P.H. Chen, C.T. Yang, Effect of viscosity of base fluid on thermal conductivity of nanofluids, *Applied Physics Letters* 93 (23) (2008) 233121-1-3.
- [54] F.D.S. Marquis, L.P.F. Chibante, Improving the heat transfer of nanofluids and nano lubricants with carbon nanotubes, *Journal of the Minerals, Metals and Materials Society* 57 (12) (2005) 32-43.

## List of Figures

1. Figure 1: TEM (200 kV) image of ‘as grown’ SWNTs from ethanol feedstock at 800°C over a Fe/Co mixture embedded in zeolite (HSZ-390HUA).
2. Figure 2: Resonant Raman spectra of ‘as grown’ SWNTs from ethanol feedstock (excitation wavelength 488 nm). The Graphite-like band (G-band), Defect induced band (D-band) and the Radial Breathing Mode (RBM) are shown. An expanded view of the RBM signals along with the diameter distribution is shown in the inset.
3. Figure 3: Structure of the sodium deoxycholate surfactant.
4. Figure 4: Comparison of thermal conductivity values measured in this work with the reference literature. Open and filled circles correspond to the measured thermal conductivity of water (top) and EG (bottom), respectively. Solid lines correspond to the literature data.
5. Figure 5: Effective thermal conductivities of SWNT/EG dispersions for different concentrations at 298 K.
6. Figure 6: Effective thermal conductivity of SWNT/EG dispersions and comparison with theoretical models [45-48].
7. Figure 7: Effective thermal conductivity of SWNT/EG dispersions, comparison with the H-S model [49] and other reported values.

Figure 1  
[Click here to download high resolution image](#)

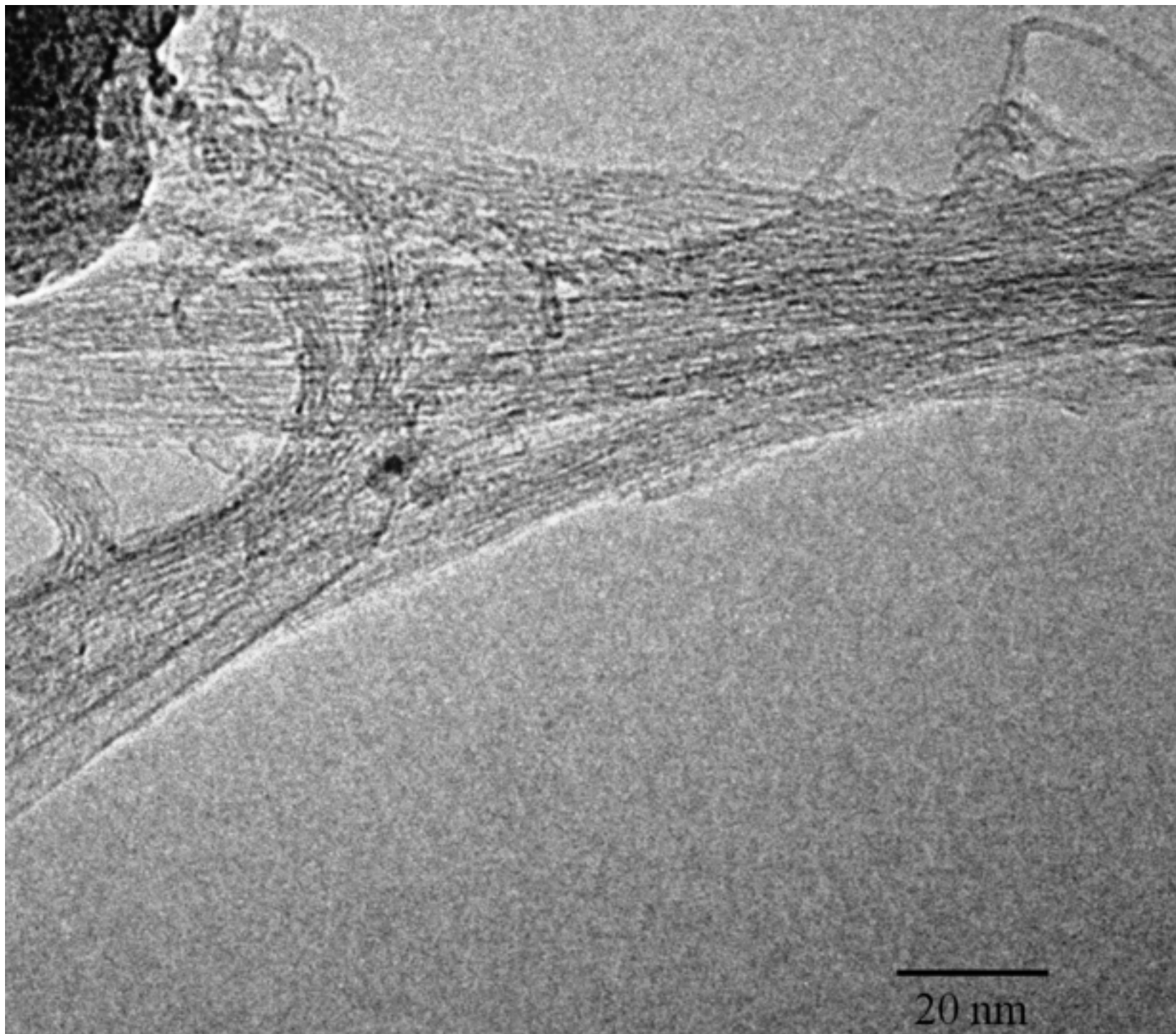


Figure 2  
[Click here to download high resolution image](#)

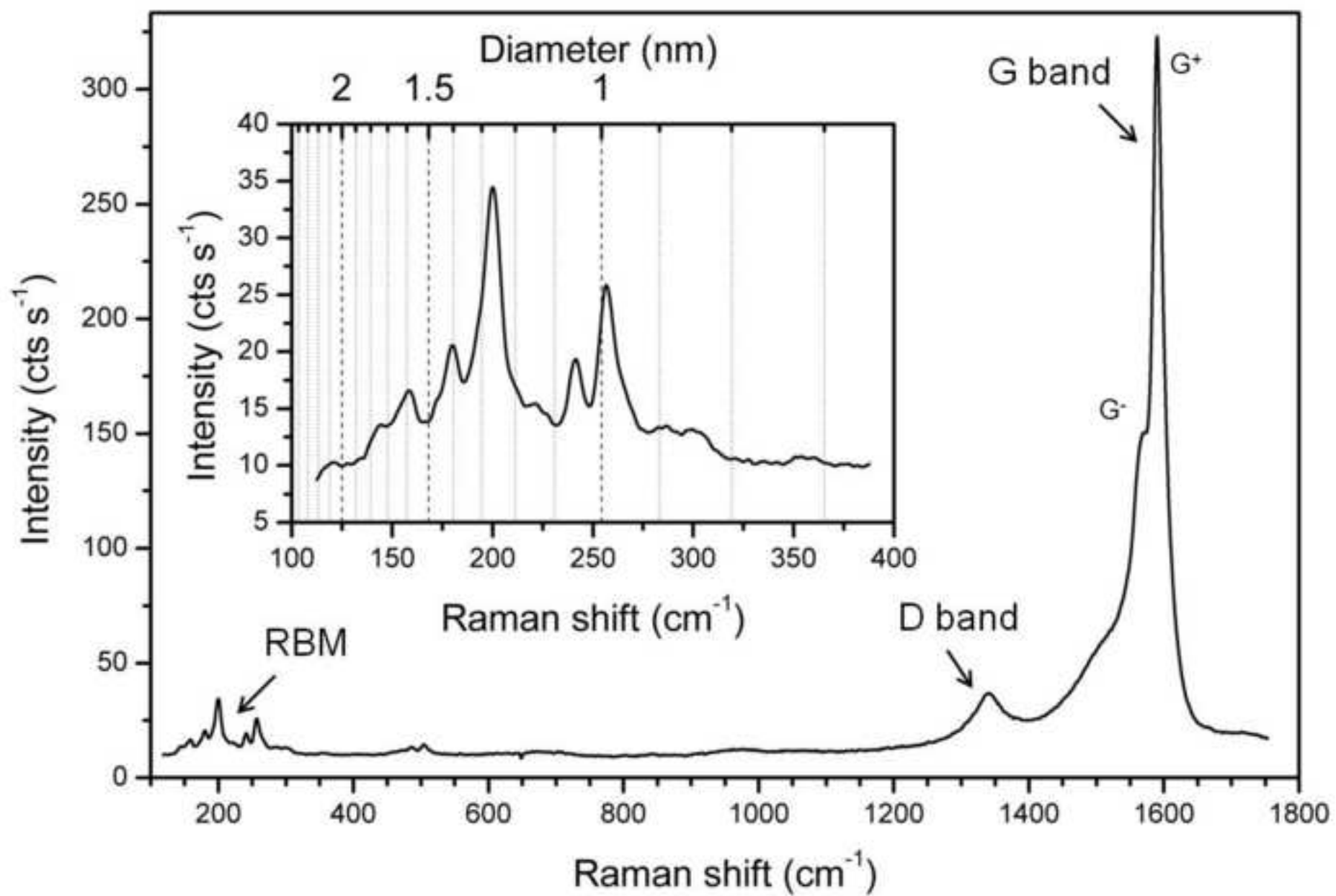


Figure 3  
[Click here to download high resolution image](#)

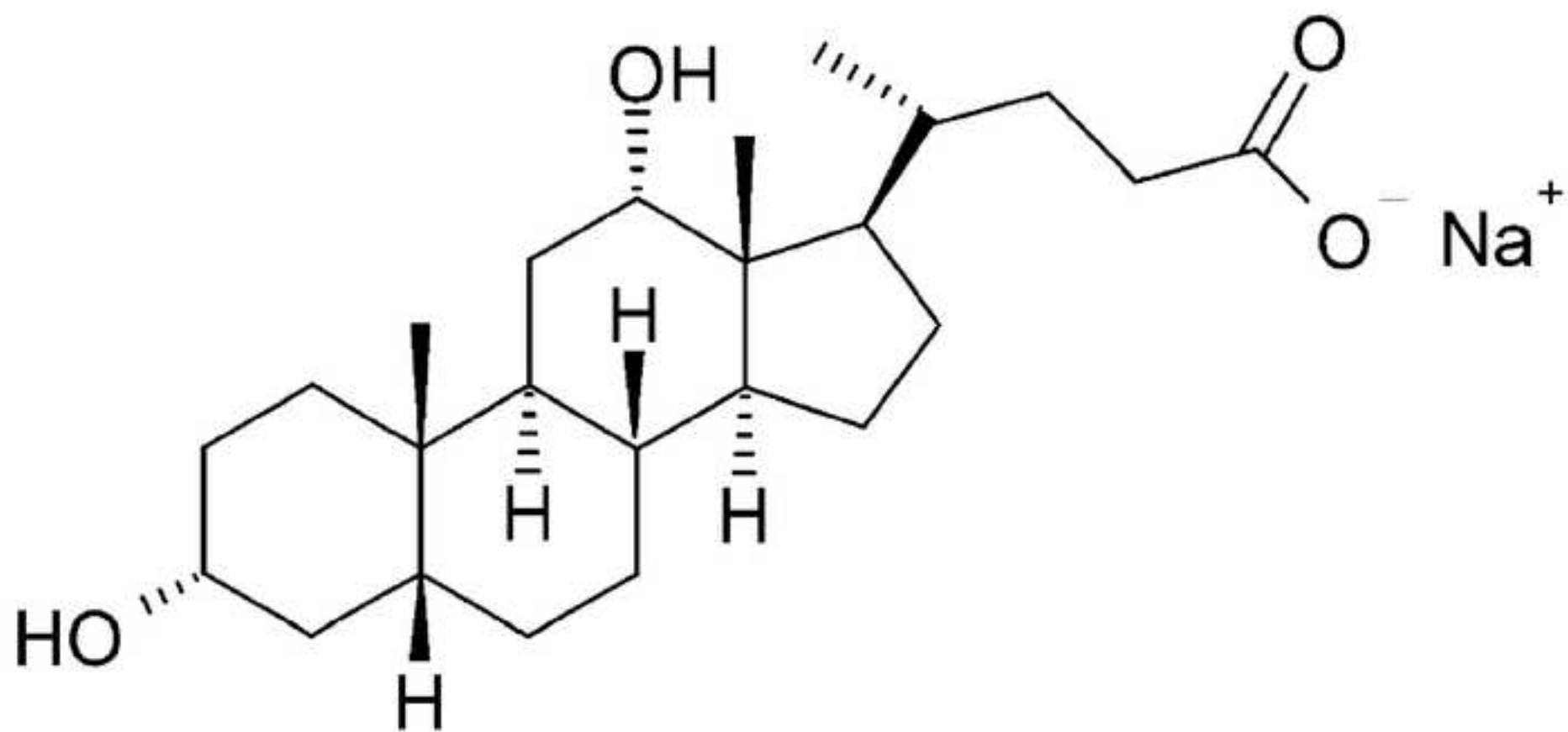


Figure 4  
[Click here to download high resolution image](#)

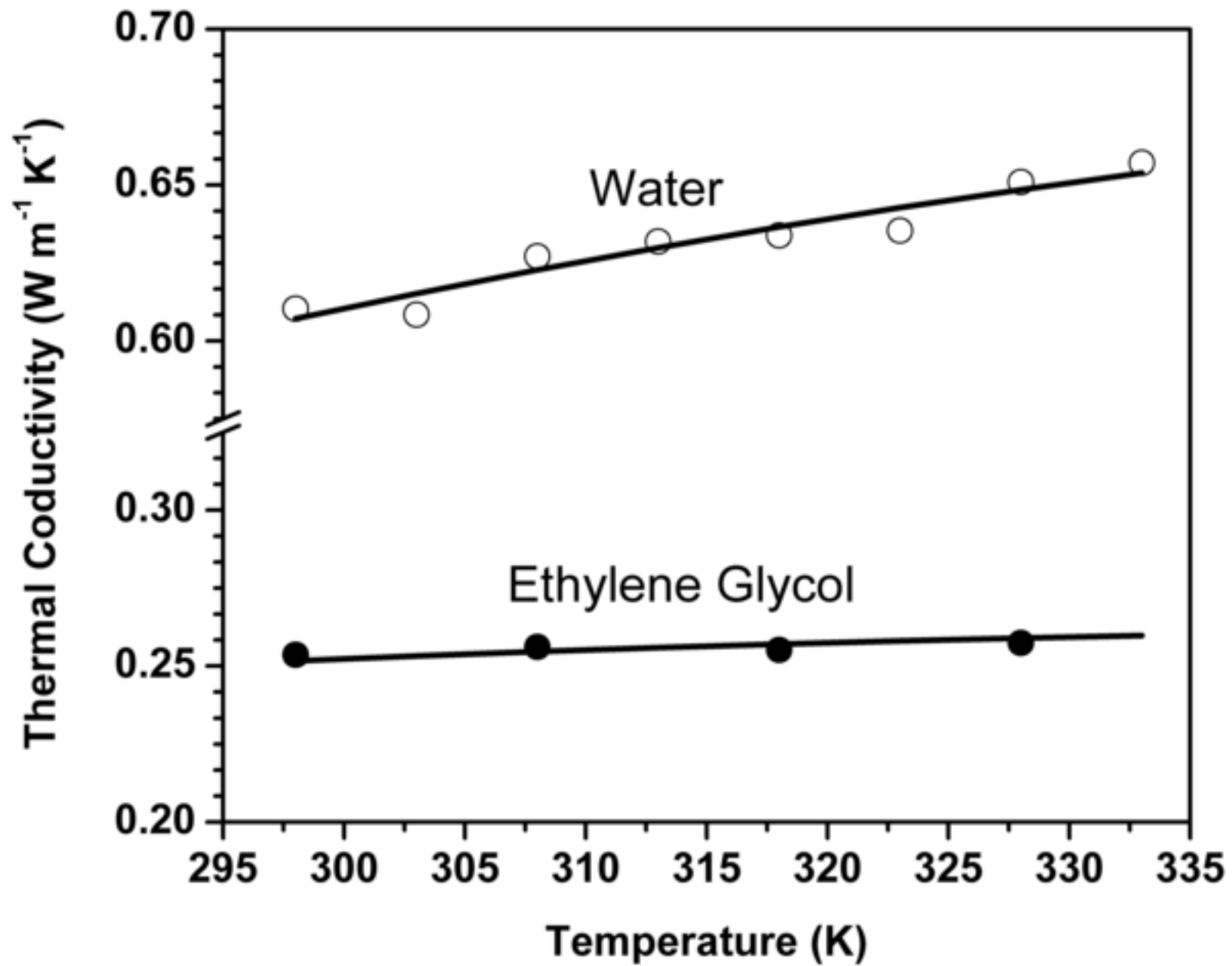


Figure 5  
[Click here to download high resolution image](#)

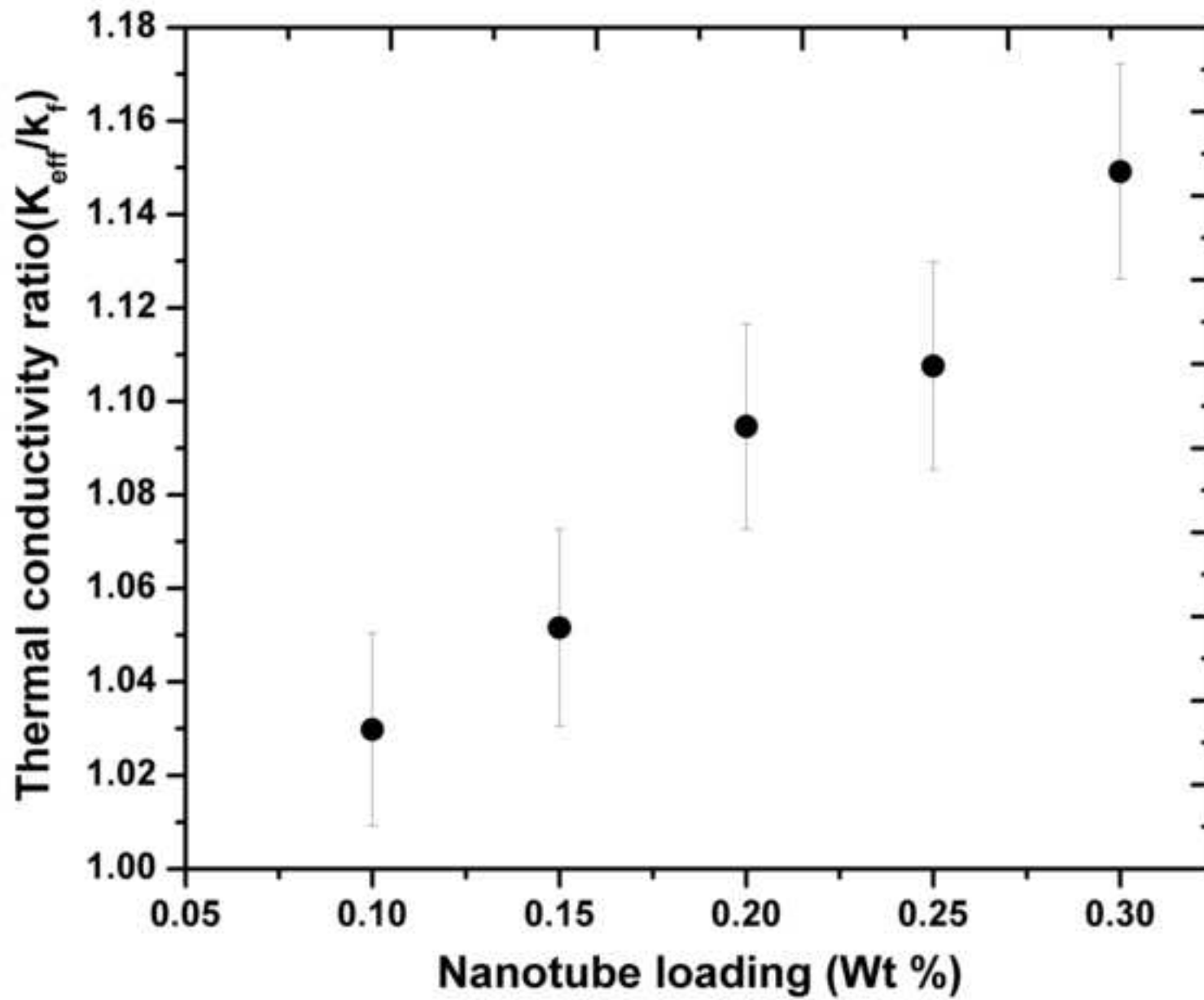




Figure 6  
[Click here to download high resolution image](#)

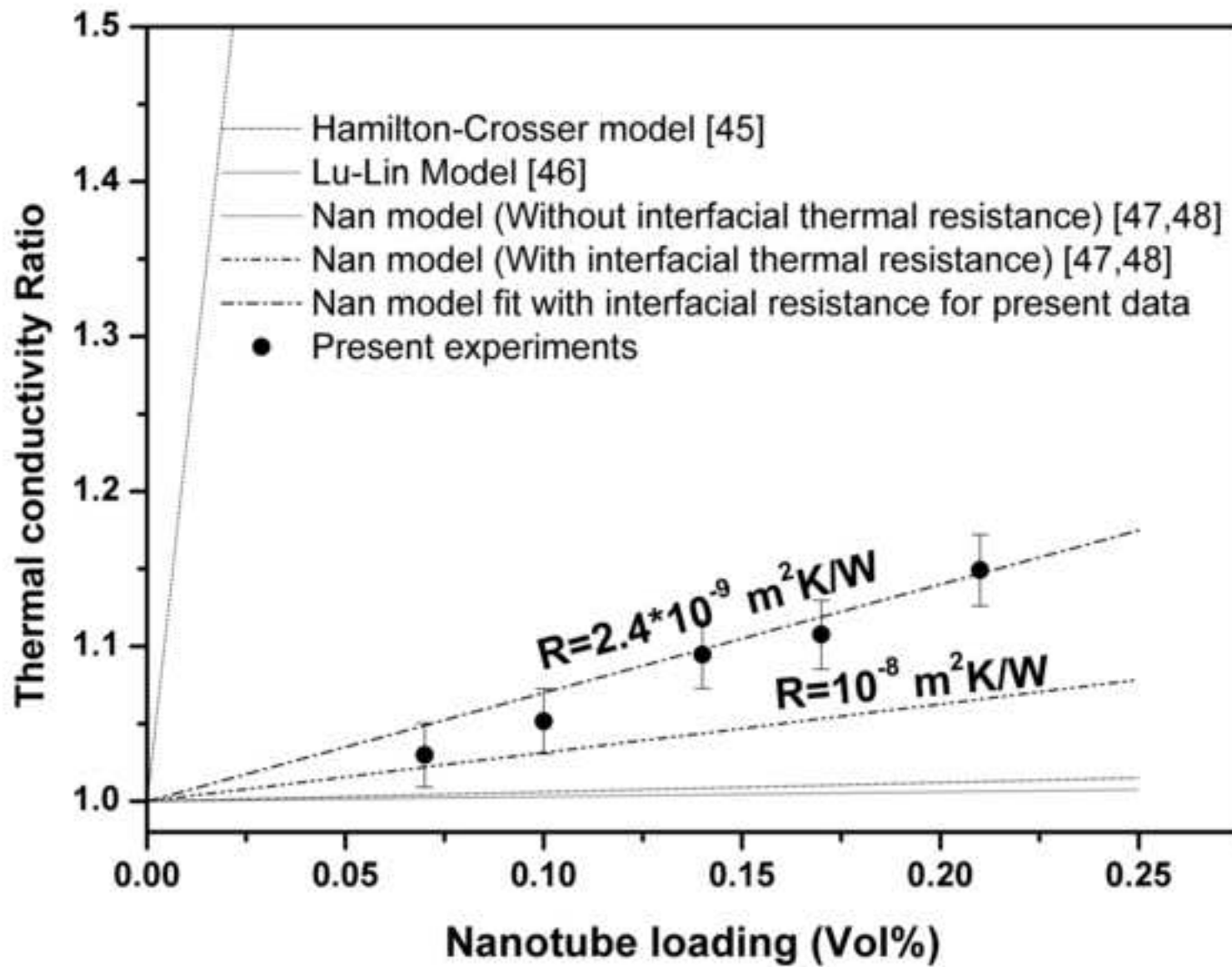




Figure 7  
[Click here to download high resolution image](#)

